Astron. Astrophys. 323, 202–210 (1997)

ASTRONOMY
AND
ASTROPHYSICS

SiO rotation-vibration bands in cool giants

I. A grid of model spectra for different stellar parameters

B. Aringer[1], **U.G. Jørgensen**[2], **and S.R. Langhoff**[3]
[1] Institut für Astronomie der Universität Wien, Türkenschanzstr. 17, A-1180 Wien, Austria aringer@astro.ast.univie.ac.at
[2] University Observatory, Juliane Maries Vej 30, DK-2100 Copenhagen, Denmark uffegj@nbivms.nbi.dk
[3] NASA Ames Research Center, Moffett Field, USA langhoff@pegasus.arc.nasa.gov

Received 10 September 1996 / Accepted 28 November 1996

Abstract. In order to study the behavior of the SiO bands of cool oxygen-rich stars we have computed a grid of 138 hydrostatic model atmospheres using an improved version of the MARCS code and new SiO line data. We found that the corresponding opacity never produces large changes of the atmospheric structure, especially if one compares it with the enormous effects from TiO or water. Based on the atmospheres, synthetic SiO spectra have been calculated with a high resolution for the photometric L-band and with a low resolution (opacity sampling) for the large wavelength range between 2.0 and 12.5 μm, which includes the fundamental as well as the first and second overtone transitions. Thus, we could study the behavior of the SiO bands as a function of different stellar parameters. It turned out that the intensity of the absorption features monotonously increases with lower temperature and gravitational acceleration as well as with higher metallicity. We expect the strongest bands in the coolest and most extended objects. When we compared our results to observations of K and M giants, we found a good agreement showing the correctness of the line data and atmospheres. On the other hand the calculations can not reproduce the relatively weak and variable bands of AGB stars indicating that our classical model atmospheres may not always work for this kind of objects. This will be discussed in a second paper, where we will focus on our observations of AGB stars.

Key words: stars: atmospheres – stars: fundamental parameters – stars: late-type – stars: AGB and post-AGB – infrared: stars

1. Introduction

Among the different molecules appearing in the atmospheres of cool oxygen-rich stars SiO is particularly interesting. Due to its high dissociation energy of 8.26 eV (Sauval & Tatum 1984) it can be found over a wide range of stellar temperatures and compared with other molecular species it is very abundant. It also represents the main condensate for the solid component in the circumstellar shells around late red giants (Gail & Sedlmayr 1986). This silicate dust produces the well known 10 μm emission observed in the IRAS LRS spectra of AGB stars (Joint Iras science working group 1986). Since the absorption features of SiO are mainly situated in the mid infrared, it may work as an efficient cooling agent (e.g. Muchmore et al. 1987) and therefore have a significant influence on the structure of stellar atmospheres. This is especially true for the hotter stars with effective temperatures between 3600 and 4600 K, because SiO is among the first molecules to be formed, whereas in the cooler objects the opacities are dominated by such species as water and TiO. However, the importance of SiO for the atmospheric cooling was recently doubted by Cuntz & Muchmore (1994).

The most important rotation-vibration bands of SiO are situated around 8 μm (ΔV = 1) and 4 μm (ΔV = 2). Especially the first overtone features can be easily accessed by ground based telescopes, since they extend into the photometric L-band. High resolution FTS spectra covering the corresponding spectral region are available for several stars allowing a detailed analysis of single lines (e.g. Ridgway et al. 1984, Tsuji et al. 1994). Nevertheless, this method is restricted to the brightest objects only. Rinsland & Wing (1982) have measured the V = 2 $\rightarrow$ 0 and V = 3 $\rightarrow$ 1 bands of a large sample of stars at a very low resolution in order to study the intensity as a function of temperature and atmospheric extension. They found that the SiO absorption is well correlated with these two parameters and may even be used as a spectral classification criterion. As they mention, this is not true for some of the latest giants, where the SiO bands show intense variations, which can not be simply explained by stellar temperature changes. Such variations have also been observed by Hinkle et al. (1976). Aringer et al. (1995) investigated the behavior of the first overtone bands in Semiregular and Mira variables using a cooled grating spectrograph at a medium resolution. They detected that despite their low temperatures many Mira stars have only a very weak or no SiO absorption, whereas all Semiregulars show strong bands. The authors interpret the

Send offprint requests to: B. Aringer

weakening of the SiO lines as a consequence of strong stellar pulsations. A correlation with temperature or properties of the circumstellar dust shells could not be found.

The purely rotational lines of SiO can be observed in the radio spectra of mass-losing late giants, where they appear in thermal as well as in maser emission (Olofsson 1988). While the thermal emission originates from the outer regions of circumstellar envelopes (e.g. Sahai & Bieging 1993) the maser lines contain information about the base of stellar winds, where the matter is accelerated and dust formation takes place (Elitzur 1992), thus providing valuable informations about these processes.

Table 1. Positions of SiO bandheads in the wavelength range between 3.96 and 4.14 μm

λ [μm]	k [cm^{-1}]	isotope	bandhead
4.0042	2497.4	^{28}SiO	V = 2 $\rightarrow$ 0
4.0292	2481.9	^{29}SiO	V = 2 $\rightarrow$ 0
4.0437	2473.0	^{28}SiO	V = 3 $\rightarrow$ 1
4.0529	2467.4	^{30}SiO	V = 2 $\rightarrow$ 0
4.0687	2457.8	^{29}SiO	V = 3 $\rightarrow$ 1
4.0838	2448.7	^{28}SiO	V = 4 $\rightarrow$ 2
4.0924	2443.6	^{30}SiO	V = 3 $\rightarrow$ 1
4.1088	2433.8	^{29}SiO	V = 4 $\rightarrow$ 2
4.1247	2424.4	^{28}SiO	V = 5 $\rightarrow$ 3
4.1326	2419.8	^{30}SiO	V = 4 $\rightarrow$ 2

2. Models and spectrum synthesis

In order to study the behavior of the SiO bands and their impact on the atmospheric structure we have calculated a grid of 138 hydrostatic model atmospheres for cool oxygen-rich stars using an improved version (Jørgensen et al. 1992) of the MARCS code (Gustafsson et al. 1975) with spherical radiative transfer routines from Nordlund (1984). We included molecular opacities of CO, TiO, H_2O and CN (Jørgensen 1994a and references therein) by treating them in the opacity sampling approximation (Jørgensen 1992). Elemental abundances for C, N and O were taken from Grevesse & Sauval (1994) otherwise from Anders & Grevesse (1989). In addition we calculated all models with and without taking into account the effects of SiO. The corresponding molecular data originate from a linelist compiled by Langhoff & Bauschlicher (1993), which represents at the moment the most accurate source of SiO opacities. The list is complete for all transitions with V $\leq$ 15 and J $\leq$ 251 for the three isotopes ^{28}Si^{16}O, ^{29}Si^{16}O and ^{30}Si^{16}O. To check the completeness of the data with respect to the total SiO opacity we calculated the vibrational-rotational partition function as a sum of all the energy levels included in the linelist and compared it with a similar partition function for all levels up to V = 29 and J = 301. The difference between the two results was less than 0.2% for T $\leq$ 4000 K. This means that the linelist is complete (in the sense of inclusion of relevant energy levels) to $\approx$ 99% for all temperatures of interest for stellar atmosphere computations. We also compared the obtained partition functions with the semi-analytical summations of Sauval & Tatum (1984) and Rossi et al. (1985). We found that the agreement is again as good as it should be expected from a high degree of completeness. We therefore conclude that neither the atmospheric structures nor the low or medium resolution spectra will be affected by spectral lines due to transitions between higher energy levels than those included in our list.

First we have produced a systematic grid of 67 atmospheres by changing the effective temperatures and gravitational accelerations in the range 2600 K $\leq$ $T_{\rm eff}$ $\leq$ 4800 K and $-0.5 \leq \log(g[cm/s^2]) \leq 4.5$ concentrating on objects with one solar mass and solar chemical abundances. The rest of the models were designed to show the effects of different masses (sphericity effects), metallicities, C/O ratios and Si abundances for several selected $T_{\rm eff}$ and log (g) values. The chosen parameters cover the following ranges: $0.6 \leq \mathscr{M}_*/\mathscr{M}_\odot \leq 9.0$, $-2.0 \leq \log(Z_*/Z_\odot) \leq 0.0$, 0.48 $\leq$ C/O $\leq$ 0.9 and 7.05 $\leq$ [Si] $\leq$ 8.05. For all our atmospheres we have adopted the solar system relative isotopic abundances of 0.9223 for ^{28}Si, 0.0467 for ^{29}Si and 0.0310 for ^{30}Si, which are taken from Anders & Grevesse (1989).

As a next step the model atmospheres were used to calculate synthetic rotation-vibration spectra for SiO. This was done with a simple radiation transport program based on the corresponding routines in the MARCS code. For observational reasons we focused on the following two items: At the beginning we worked on high and medium resolution spectra covering the short wavelength part of the first overtone transitions and then we calculated low resolution spectra (opacity sampling resolution) for the whole infrared range between 2.0 and 12.5 μm including all ΔV = 1, 2 and 3 bands.

To study the behavior of the first overtone bands we produced synthetic spectra for the wavelength range between 3.96 and 4.14 μm. This region is interesting, because it covers the existing SiO observations in the L-band (e.g. Rinsland & Wing 1982, Aringer et al. 1995) and it can be easily accessed by future ground based measurements. It contains the short wavelength part of the first overtone transitions starting with the V(2,0) feature of ^{28}SiO at approximately 4 μm. An overview including all SiO bandheads in the selected range is given in Table 1. The model spectra have been calculated with a very high resolution of R = 400000, which is enough for a good description of the line shapes. The latter were assumed to be simple Doppler profiles, since we did not attempt any exact fit to results from high resolution FTS spectroscopy. In addition, especially close to the bandheads, the wings of even the strongest lines will often be weaker than the Doppler cores of the many overlapping neighboring ones. On the other hand many of the SiO lines are extremely saturated in the atmospheres of cooler giants causing especially their width, which is mainly determined by the microturbulence (ξ), to have a strong influence on medium and low resolution work. As a consequence the intensity of the SiO absorption depends much on the value of ξ (This is also the reason, why the resolution must be high enough for representing the line profiles well.). For our grid of synthetic spectra we have adopted ξ = 2.5 km/s, which is consistent with the opacity

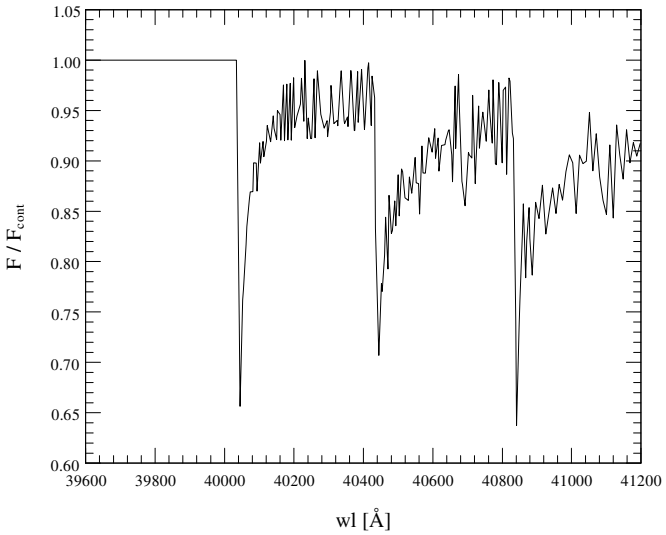

Fig. 1. Medium resolution SiO spectrum (R $\sim$ 4000) for the wavelength range from 3.96 to 4.12 μm. The stellar parameters are $T_{\rm eff}$ = 3600 K, $\log(g[{\rm cm/s^2}]) = 0.0$, ξ = 2.5 km/s, solar mass and chemical abundances. The continuum is set to one and only SiO lines are included. For an identification of the bandheads see Tab. 1.

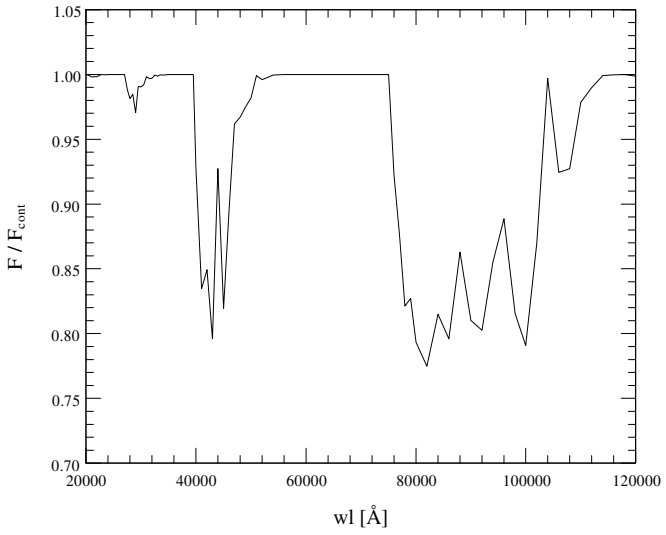

Fig. 2. Low resolution SiO spectrum (R $\sim$ 50) for the wavelength range from 2.0 to 12.0 μm. The stellar parameters are $T_{\rm eff}$ = 3600 K, $\log(g[{\rm cm/s^2}]) = 0.0$, ξ = 2.5 km/s, solar mass and chemical abundances. The continuum is set to one and only SiO opacities are included. The fundamental, first and second overtone bands can be seen.

sampling data used for the model atmospheres. In addition we have varied ξ for several selected stellar parameters between 1.0 and 6.0 km/s to investigate the effect of different line widths.

In Fig. 1 we present a typical result of our calculations. This is a medium resolution SiO spectrum (R $\sim$ 4000) of an AGB star, which was simply derived by averaging over the points from the synthetic data. It shows the wavelength range from 3.96 to 4.12 μm. The continuum is set to one and the corresponding stellar parameters are $T_{\rm eff}$ = 3600 K, $\log(g[{\rm cm/s^2}]) = 0.0$, $\mathcal{M}_* = 1.0\,\mathcal{M}_\odot$, $\log(Z_*/Z_\odot) = 0.0$, C/O = 0.48, [Si] = 7.55 and ξ = 2.5 km/s (C/O and [Si] solar). One can clearly see most of the different bandheads mentioned in Table 1. It is also obvious that the absorption of the main isotope ^{28}SiO can be very strong in cool objects.

In order to compare the intensity of different band systems we created for all model atmospheres synthetic spectra covering the wavelength range between 2.0 and 12.5 μm, which includes the fundamental as well as the first and second overtone transitions. Because of very practical reasons like calculation time and disk space this could only be done at a rather low resolution. Although such an approach does not allow to resolve line profiles, which is necessary for describing the SiO absorption correctly, one can still obtain realistic results by using the opacity sampling approximation that has already been applied for the model atmospheres. Fig. 2 shows a spectrum derived by this method adopting the same stellar parameters as in Fig. 1. The continuum is again set to 1 and only SiO features are included. The original resolution of R $\sim$ 500 (between R $\sim$ 1000 at 2 μm and R $\sim$ 200 at 10 μm; approximately equidistant stepsize in wavenumber) was reduced to a value of R $\sim$ 50, because due to its statistical nature the opacity sampling approximation only gives correct results, if one takes the average of a larger number of spectral points. But in the case of the SiO band systems this is still enough to determine their total intensity.

3. Results

3.1. Influence of SiO on stellar atmospheres

As mentioned in the previous section, we have calculated all model atmospheres with and without taking into account the opacity of SiO. By comparing the results it became possible to estimate, how important this molecule is for the atmospheric structure. Fig. 3 displays a temperature versus pressure plot for an object with $T_{\rm eff}$ = 3400 K, $\log(g[{\rm cm/s^2}]) = 0.0$, solar mass and chemical composition. In addition to the models with and without SiO we also show the curve for an atmosphere that has been calculated neglecting the opacities of TiO as well as of SiO. This allows to compare the effects of those two molecules. As one can clearly see, the presence of TiO causes a substantial heating over a large region of the atmosphere. This is related to the fact that its strong bands are generally located at wavelengths shorter than the spectral maximum of the stellar radiation field (Gustafsson & Jørgensen 1994). On the other hand SiO with its main rotation-vibration transitions in the mid infrared tends to cool the surface layers and gives rise to a corresponding small back-warming effect, which is seen in Fig. 3 for regions deeper than about $P_g \sim 10\,{\rm dyn/cm^2}$.

Another obvious result from Fig. 3 is that the influence of SiO remains small in all layers, especially if one compares it with the enormous changes produced by TiO (shown) or H_2O, the latter being important in cooler stars. As one can see, the corresponding temperature differences never exceed 50 K, although this is one of the models with the strongest effects from SiO. If all other atmospheric parameters are kept constant, the

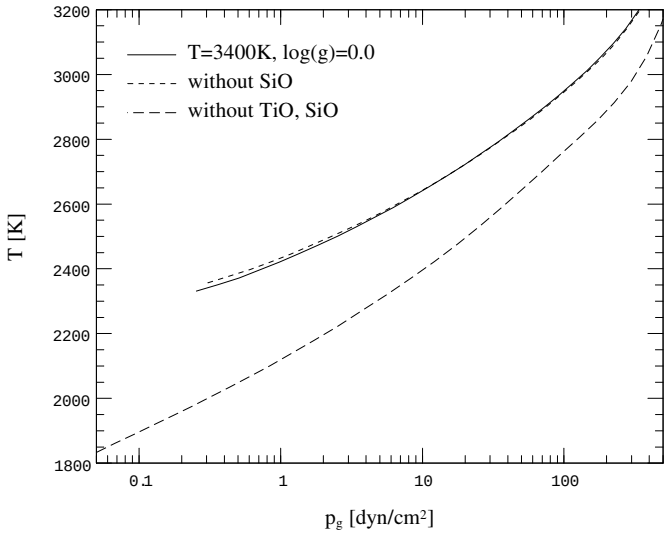

Fig. 3. The atmospheric temperature-pressure structure for T_{eff} = 3400 K, log (g[cm/s^2]) = 0.0, solar mass and chemical composition. The three different curves have been computed including all available molecular opacities (full line), neglecting the opacities of only SiO (short dashes) and neglecting the opacities of TiO and SiO (long dashes). The largest changes are seen to be due to TiO.

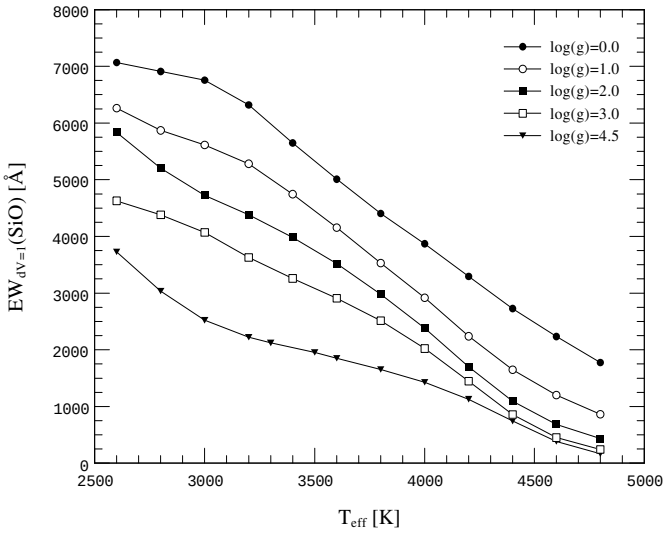

Fig. 4. The total equivalent width of the SiO fundamental band ($EW_{\Delta V=1}$ (SiO)) as a function of effective temperature and gravitational acceleration for stars with solar mass and abundances. log (g) is in units of [cm/s^2].

temperature differences always decrease monotonously with growing values of log (g), which is due to a general weakening of the SiO bands (see next subsection). As a consequence the SiO molecule has practically no influence on objects with log (g[cm/s^2]) $>$ 2.0. The same is also true for stars with $T_{eff} > 4000$ K or $T_{eff} < 3000$ K. If the temperatures become too high, the SiO bands will be too weak to cause any significant changes of the atmosphere. On the other hand it turns out that in very cool objects the opacity is completely dominated by TiO and H_2O, while SiO only plays an unimportant role. The strongest effects from SiO appear in stars with log (g[cm/s^2]) $\leq$ 0.0 and 3200 K $\leq T_{eff} \leq$ 3600 K. But even in these models we have never found temperature changes exceeding 50 K, which allows us to conclude that the influence of SiO on the atmospheric structure of cool stars remains always small as long as hydrostatic and chemical equilibrium can be assumed.

3.2. The intensity of SiO bands as a function of temperature and atmospheric extension

In order to investigate the behavior of the intensity of the SiO absorption we have calculated equivalent widths for several of the corresponding molecular features using our synthetic spectra. The following bandheads have been measured from our high resolution data: V = 2 $\rightarrow$ 0 of ^{28}SiO (λ = 4.0025 − 4.0200 μm), V = 3 $\rightarrow$ 1 of ^{28}SiO (λ = 4.0425 − 4.0600 μm), V = 4 $\rightarrow$ 2 of ^{28}SiO (λ = 4.0825 − 4.1000 μm), V = 2 $\rightarrow$ 0 of ^{29}SiO (λ = 4.0265 − 4.0350 μm) and V = 3 $\rightarrow$ 1 of ^{29}SiO (λ = 4.0665 − 4.0750 μm). As one can see in Tab. 1, the wavelength ranges defined to study the V = 3 $\rightarrow$ 1 and V = 4 $\rightarrow$ 2 bands of ^{28}SiO also include ^{30}SiO features. But since the latter are comparatively weak, they show no significant influence on the results. This is not true for the absorption caused by the main isotope and extending into the spectral windows used to measure the ^{29}SiO bandheads. As a consequence the corresponding equivalent widths will always depend on both of these two features. In addition we have determined the total intensity of the whole ΔV = 1 (λ = 7.4 − 12.0 μm) and 2 (λ = 3.8 − 5.5 μm) bands from our low resolution spectra.

In Figs. 4 and 5 we present the intensity of the SiO absorption as a function of stellar temperature for different values of log (g). In Fig. 4, which displays the total equivalent width of the whole fundamental band ($EW_{\Delta V=1}$ (SiO)), one can see that the latter decreases monotonously with T_{eff}, if the gravitational acceleration remains constant. This trend is almost linear. Only for the coolest objects and the smallest log (g) values there seems to be some saturation effect. The situation is a little bit different for the sum of the equivalent widths corresponding to the V = 2 $\rightarrow$ 0, V = 3 $\rightarrow$ 1 and V = 4 $\rightarrow$ 2 bandheads of the main isotope, which is shown in Fig. 5 and will be called EW_L (SiO) in the following text (L for the photometric L-band). As for the fundamental band, the SiO absorption always goes monotonously down with the temperature. But for the more extended atmospheres there appears a very strong decrease between T_{eff} = 3200 K and 4200 K, while the gradient is only weak for cooler and hotter stars. This behavior causes the curves to show some kind of "s-shape". It is not so well pronounced in objects with log (g[cm/s^2]) $\geq$ 2.0, where the decrease is much more linear. For the most compact atmospheres the largest gradient even seems to appear at $T_{eff} < 3000$ K.

In Figs. 4 and 5 it is also obvious that at every temperature the SiO absorption becomes smaller, if the gravitational acceleration grows. As it turned out in all of the investigated cases,

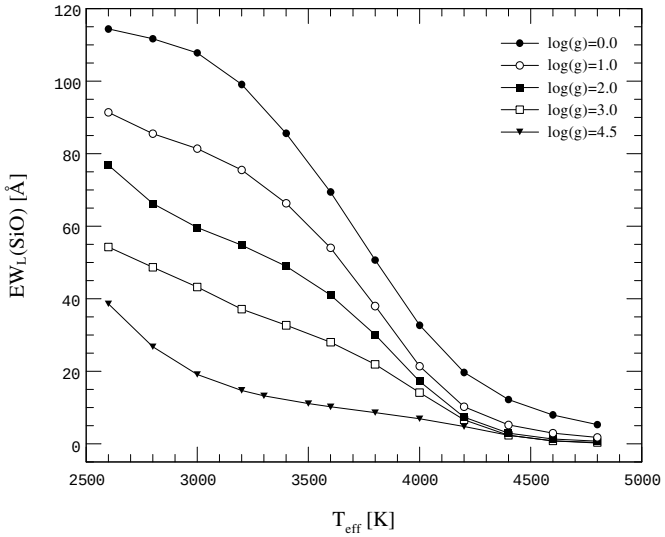

Fig. 5. The sum of the equivalent widths of the V = 2 → 0, V = 3 → 1 and V = 4 → 2 bandheads of the main SiO isotope (EW_L (SiO)) as a function of effective temperature and gravitational acceleration for stars with solar mass and abundances. log (g) is in units of [cm/s^2].

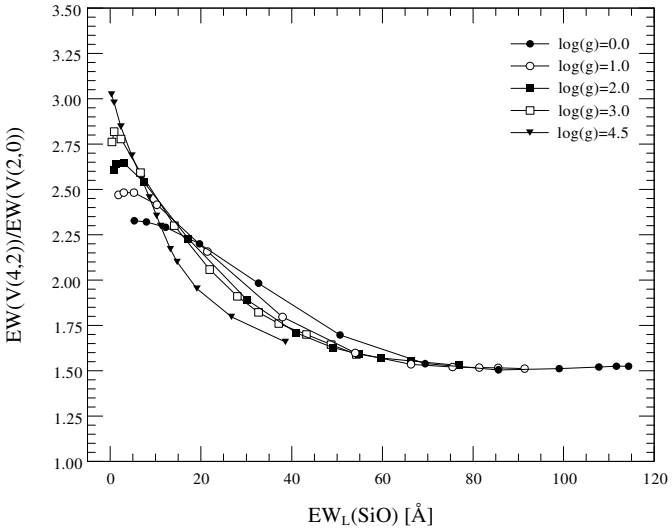

Fig. 6. The ratio EW (V = 4 → 2)/EW (V = 2 → 0) as a function of the SiO absorption in the photometric L-band (EW_L (SiO)) for different gravitational accelerations. Solar mass and abundances are assumed. log (g) is in units of [cm/s^2].

the relation between the equivalent width of the SiO bands and log (g) is almost linear. Thus, the strongest SiO features are expected in very cool giants and supergiants, while they always will be relatively weak in dwarfs.

From our observations of AGB stars (Aringer et al. 1995) we found that the intensity ratios of the SiO bandheads show a large scatter, if different objects are compared. For example, in our sample the value of EW (V = 4 → 2)/EW (V = 2 → 0) changes by a factor of more than 2. This is partly related to the total amount of the SiO absorption. But even if the latter remains constant, there is still a considerable scatter left, which may be caused by a different T_{eff} or log (g). In principle the ratio between the intensities of any band originating from transitions to the V = 0 level and its hot bands (transitions involving only vibrationally excited levels) will reflect the temperature at the depth(s) of formation in the stellar atmosphere (primarily via the Boltzmann factor). Since the latter may be a function of T_{eff} and log (g), those parameters could also affect the intensity ratios. In order to see, if this is true and if the SiO features can be used for an independent determination of effective temperature and gravitational acceleration, we compared the equivalent widths (EW) of some bandheads. First we concentrated on the ^{28}SiO transitions in the photometric L-band. Fig. 6 displays a plot of the ratio EW (V = 4 → 2)/EW (V = 2 → 0) as a function of the sum EW_L (SiO), which represents a good measure for the SiO absorption in this range. It is obvious that EW (V = 4 → 2)/EW (V = 2 → 0) decreases with growing EW_L (SiO) in objects showing weak features, while it remains approximately constant at EW_L (SiO) > 40 Å. The symbols and curves correspond to different gravitational accelerations. As one can see, the latter do not produce any systematic trends or larger deviations from the overall relation. The same also applies to the effects caused by temperature variations, and the other ratios like EW (V = 3 → 1)/EW (V = 2 → 0) show a similar behavior. Thus, we must conclude that the ^{28}SiO bandheads in the photometric L-band alone are not a good tool for an independent measurement of T_{eff} and log (g), as long as one works with low or medium resolution spectroscopy. Their ratios are almost only a function of the total intensity of the SiO absorption in this wavelength range, especially if one takes into account that there are always uncertainties in the observations and atmospheric models.

The last two statements are also valid, if the study is extended to the bandheads of the isotope ^{29}SiO. For example, the ratio EW (^{29}SiO)/EW (^{28}SiO) for the V = 2 → 0 transition increases with EW_L (SiO), and the scatter around the corresponding relation, which is almost linear, remains very small. On the other hand this may offer an advantage, because it could make it easier to estimate the isotopic abundances.

Finally we have compared the total intensities of the fundamental and the first overtone bands. It turned out that for T_{eff} < 3600 K the ratio is almost independent of temperature and only determined by variations of the gravitational acceleration: For higher values of log (g) the ΔV = 2 transitions become weaker relative to the ΔV = 1 features. On the other hand, if the atmospheres become hotter than 3600 K, there exists no clear trend being caused by different values of either T_{eff} or log (g). Of course, the ratio of the equivalent widths is also correlated with the total intensity of the SiO absorption (in all bands). But the scatter around the corresponding relation is very large. However, there are again no systematic trends caused by temperature or gravitational acceleration.

3.3. Sphericity effects

Since we have calculated our synthetic atmospheres using spherical radiation transport routines, we are able to investigate deviations from plane parallel geometry. The latter are related to the fact that the structure of spherical models is a function of stellar mass (as oppose to the plane parallel models). As one would expect, we found the strongest sphericity effects in the SiO features of the most extended and least massive stars. On the other hand, for objects with high mass and/or gravity the spherical models approach the plane parallel ones. To give some typical numbers, for $\log(g[cm/s^2]) = 0.0$ and solar chemical abundances the ratio between EW_L (SiO) for a $0.6\,\mathscr{M}_\odot$ and for a $9.0\,\mathscr{M}_\odot$ star (which is almost plane parallel) varies from 1.02 to 1.6, the largest values corresponding to the highest effective temperatures. In objects with $\log(g[cm/s^2]) \geq 1.0$ the sphericity effects never produce significant changes of the SiO opacities. This demonstrates that the intensity of the SiO features decreases as a function of stellar mass, although the effect does not become very important, since larger differences appear only in hotter models, where the bands are already weak. And in high gravity stars deviations from plane parallel geometry can be completely neglected.

3.4. Chemical abundances

It is evident that changes of the chemical abundances may have a large impact on the formation of SiO and consequently on the appearance of the SiO features. Therefore we studied such effects starting with the metallicity. In Fig. 7, which presents EW_L (SiO) as a function of $\log(Z_*/Z_\odot)$, the different curves and symbols correspond to selected temperatures and gravitational accelerations. One can see that for all parameters the intensity of the bandheads increases steadily with log (Z) showing almost a linear growth. This means that stars belonging to the galactic population II will always have much weaker SiO features than those with solar metallicity.

A similar and also very strong effect can be obtained, if one changes only the silicon abundance, which is shown in Fig. 8. As a consequence in principle it should be possible to estimate this quantity from low or medium resolution spectroscopy in the photometric L-band. But in practice it is not that simple, because the intensity of the SiO bands also depends on T_{eff}, log (g) and log (Z), which are in general not precisely known, especially for the coolest giants.

Finally, we have also investigated the effects of variations in the C/O ratios. Such changes may occur in AGB objects, when they transform into carbon stars (e.g. Lambert 1994). We studied the range between $C/O = 0.48$ (solar) and 0.9. We did not go to higher values, since it is not likely that the used chemical equilibrium routine still gives correct results, if one comes too close to $C/O = 1$. This is due to the neglect of typical S-type molecules like VO, YO, ZrO and LaO. For $C/O > 1$ there will be a carbon rich environment, where almost no SiO forms (Jørgensen 1994b). Within the limits of our investigation, which covered only values of T_{eff} and log (g) that are typical for AGB

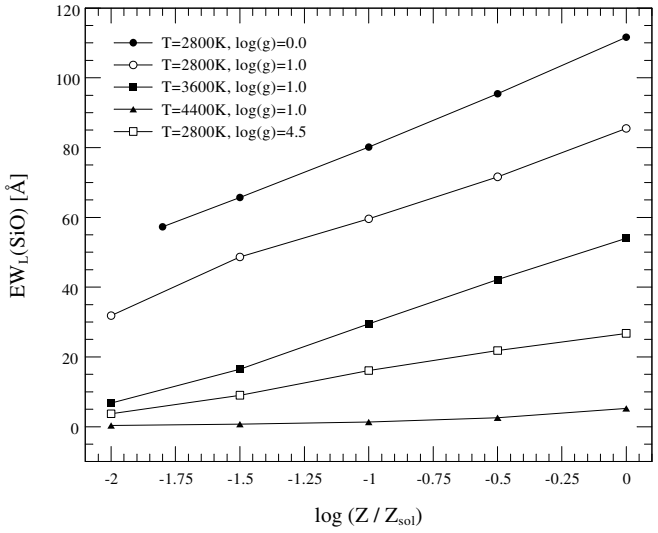

Fig. 7. The equivalent width of the V = 2 → 0, V = 3 → 1 and V = 4 → 2 bandheads of the main SiO isotope (EW_L (SiO)) as a function of metallicity for different effective temperatures, gravitational accelerations and for one solar mass. log (g) is in units of $[cm/s^2]$.

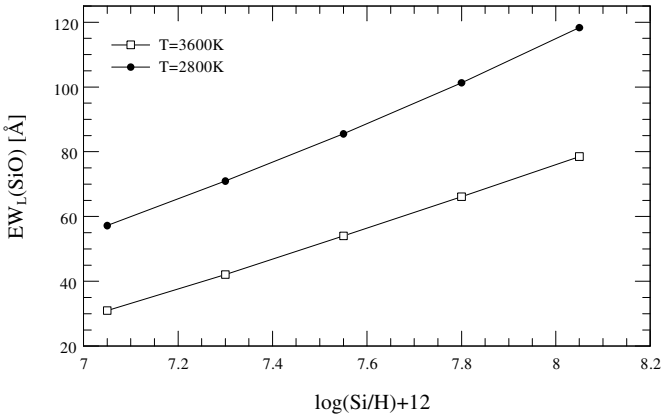

Fig. 8. The equivalent width of the V = 2 → 0, V = 3 → 1 and V = 4 → 2 bandheads of the main SiO isotope (EW_L (SiO)) as a function of the silicon abundance for T_{eff} = 2800 and 3600 K, $\log(g[cm/s^2]) = 1.0$ and one solar mass.

stars, we did not find any systematic or strong variations of the SiO bands, reflecting that the SiO density is determined by the silicon abundance only. For some models there was a slight decrease with C/O and for others we even observed an increase. The latter may be due to changes of the atmospheric structure.

3.5. Microturbulence

As it has already been mentioned in the previous section, the appearance of the SiO bands at a low or medium resolution is also influenced by the microturbulence. In general their intensity increases, if the value of ξ becomes larger, since many of the lines are saturated. As one would expect, the size of this effect depends on the original intensity of the SiO absorption

and the most striking changes can be found for the very cool and extended atmospheres. For example, in an object, which is characterized by T_{eff} = 2800 K, $\log(g[cm/s^2])$ = 0.0, solar mass and chemical abundances, EW_L (SiO) grows by a factor of approximately 2, if ξ increases from 1.0 to 3.5 km/s. Of course, this is one of the models with the strongest variations. The corresponding value for a similar star with T_{eff} = 3600 K is still almost 2, but it drops quickly at higher temperatures. On the other hand, if EW_L (SiO) is smaller than 20 Å, the influence of the microturbulence remains always negligible. Thus, one has only to worry about the ξ values of very cool giants and supergiants.

4. Discussion

In this section we want to compare our results to other work done on the SiO features of late type giants. First we start with the observations from Rinsland & Wing (1982), who investigated the V = 2 → 0 and V = 3 → 1 bandheads at 4 μm. Their spectra have only a rather low resolution of about 500, but they cover a large number of objects allowing a study of stars with very different properties. In Fig. 9 we compare their measurements to our calculations showing the equivalent widths as a function of spectral type. As one can see, the agreement between observations and models is quite good, especially if one takes into account the uncertainties of the stellar parameters. The plot includes mainly III-giants, since we could determine their effective temperatures and gravitational accelerations as a function of spectral type using different measurements of angular diameters taken from the literature and estimating their mass (Blackwell et al. 1990, Bonnell & Bell 1993, Di Benedetto & Rabbia 1987, Drake & Smith 1991, Ridgway et al. 1982). This is much more difficult for the very luminous stars. Nevertheless, also for a few of these objects – like α Ori – it was possible to compare our results to the data from Rinsland and Wing. And the agreement was again satisfactory. Unfortunately, this is not true for the very extended coolest giants with $T_{eff} < 3500$ K, where the predicted SiO absorption is always much stronger (50 % and more) than the observed one. As an example we have included the II-giants β Peg and ρ Per in Fig. 9, the latter being a semiregular variable and most probably also an AGB star, which is the case for many of these objects. The situation becomes even worse, if one looks at Mira, where Rinsland and Wing found an intense variation of the SiO bands connected to the stellar pulsation. Sometimes this causes the features almost to disappear. Of course, such a behavior can not be explained by our hydrostatic models. Even if temperature changes are taken into account, we never get a complete extinction of the SiO features.

Aringer et al. (1995) observed the first overtone bands of supposed AGB stars at a medium resolution of approximately 4000. Their spectra cover the wavelength range between 3.95 and 4.10 μm including the V = 2 → 0, V = 3 → 1 and V = 4 → 2 bandheads of the main isotope. They investigated a sample of 23 oxygen-rich very cool giants, which are mainly Mira and semiregular variables. Confirming the results from

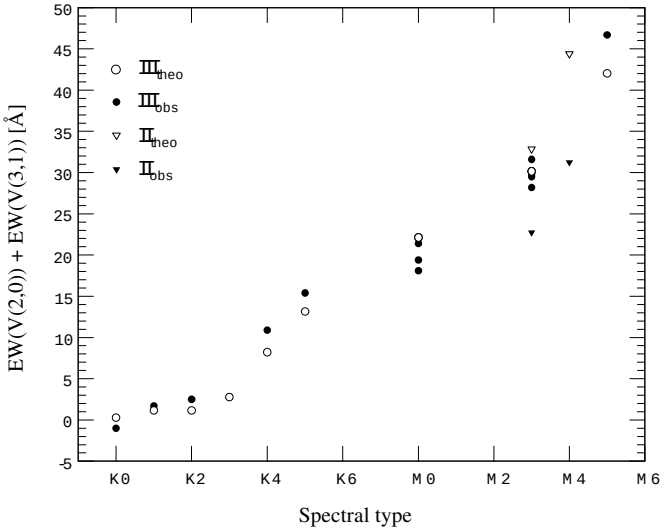

Fig. 9. The equivalent widths of the V = 2 → 0 and V = 3 → 1 bandheads of the main SiO isotope, which have been measured by Rinsland and Wing (1982) for K and M giants (full symbols), are compared to our theoretical values (open symbols). They are presented as a function of spectral type for class III (circles) and II (triangles). The corresponding effective temperatures and gravitational accelerations are taken from the literature (see text). One can see that the agreement between observations and models is quite good for the III-giants, whereas the predicted bands of the II-giants are too strong.

Rinsland and Wing they found that many Mira stars have only a weak or no SiO absorption. They also suspect a connection with the stellar pulsation, since the semiregular variables with their much smaller photometric amplitudes always show strong SiO features. In addition there seems to be a correlation between the disappearance of the bands and the occurrence of Brackett-α emission, which is caused by shocks propagating through the atmosphere. The latter are also a consequence of stellar pulsation. However, even the strongest bands measured by Aringer et al. are still much weaker than our predictions for the effective temperatures and gravitational accelerations usually related to AGB stars. Thus, it is again confirmed that hydrostatic equilibrium models do not work for this type of objects. A detailed discussion of the observations by Aringer et al. will be given in the second paper of this series. A possible explanation for the comparatively weak SiO bands in AGB stars is the impact of dynamical atmospheres. Unfortunately, a self-consistent description of the different phenomena like pulsation, mass loss and dust formation including also molecular opacities does not exist at the moment. But it may be possible to calculate exploratory spectra based on available simple (concerning opacities and coupling of the phenomena) models (e.g. Höfner & Dorfi 1997) in order to estimate the effects.

It should be mentioned that the discrepancies between our models and the observations of AGB stars can not be explained by a wrong value of ξ. In order to get the right intensities one needs microturbulent velocities of less than 1 km/s, which is in

contradiction with high resolution measurements. Our adopted ξ of 2.5 km/s seems to be appropriate (e.g. Tsuji et al. 1994).

Although it was not our aim to reproduce detailed line profiles, we have compared our results to several selected high resolution spectra (Ridgway et al. 1984, KPNO FTS archive). As a typical example we show in Fig. 10 FTS data for the K5III giant α Tau and a corresponding synthetic SiO spectrum, which has been calculated assuming a model atmosphere with $T_{\rm eff}$ = 3900 K, log (g[cm/s^2]) = 1.0, $\mathcal{M}_* = 1.0\,\mathcal{M}_\odot$ and solar chemical abundances. These values are very close to the real properties of the star (Bonnell & Bell 1993, Di Benedetto & Rabbia 1987, Ridgway et al. 1982), which is also true for our adopted ξ of 2.5 km/s. The plot covers two different wavelength ranges one including the V = 4 $\rightarrow$ 2 bandhead of ^{28}SiO and the other one situated in a region with just a few strong SiO lines. Taking into account the uncertainties of the stellar parameters, the presence of spectral features produced by other species in the stellar as well as in the Earth's atmosphere and our simple treatment of the line profiles (see sect. 2) the agreement between the FTS data and our calculation is satisfactory. Similar results were also obtained for other K and early M giants (e.g. α Boo), whereas it was again not possible to reproduce the spectra of very extended and cool objects, because the predicted SiO absorption for those stars came out too strong. In Fig. 10 there seems to be some discrepancy concerning the line widths, since our lines generally appear narrower than the observed ones. This may be due to the lower resolution of the FTS spectra ($\sim$ 100000) and the already mentioned simple treatment of the profiles, which could also cause an underestimation of the intensity for the outermost edge of the bandheads, where the density of the lines is extremely high. Nevertheless, this will have almost no influence on the appearance of medium or low resolution spectra (i.e. it could be simulated by a small change of ξ).

In a recent paper Tsuji et al. (1994) analysed high resolution FTS data of the SiO first overtone lines of six late type M giants and two M supergiants. They determined silicon abundances and isotopic ratios by using several different methods including a semi-empirical curve-of-growth analysis and synthetic spectra from model atmospheres. Since their work is dedicated to the study of individual lines, their fits to the profiles are much better than ours. However, they were also not able to reproduce the intensities for the most extended and coolest objects (e.g. RX Boo), although the discrepancies appear to be smaller than in our case and they could even reproduce the observed spectrum of the semiregular variable R Lyr. But this is caused by the fact that they used f-values, which are too weak compared to the new data by Langhoff & Bauschlicher (1993) (see also the appendix in Tsuji et al.). As a consequence, their adopted silicon abundances have to be decreased by a factor of around two in order to fit the observed spectra without any changes in the atmospheric parameters. This causes the values to be sub-solar for the late M giants. On the other hand our work has shown that there are still a lot of problems concerning the model atmospheres of cool extended stars making the interpretation of spectral data very difficult. And this is especially true for the determination of absolute chemical abundances, although in principle the SiO bands may be a very good indicator for silicon, as we have demonstrated in the last section.

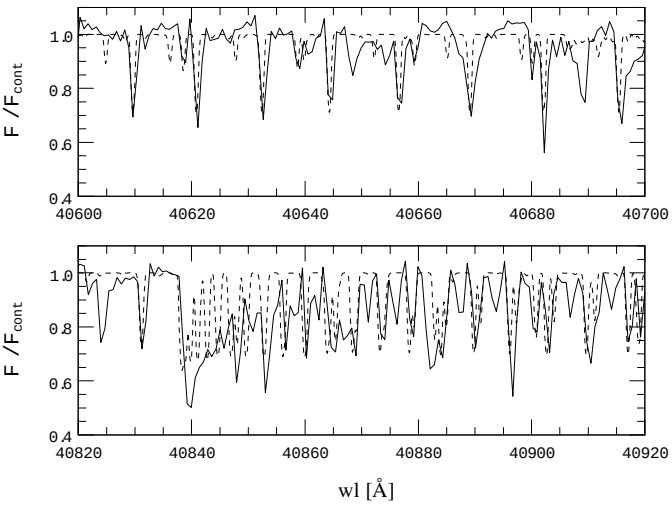

Fig. 10. The observed high resolution spectrum of α Tau (full line) and a synthetic SiO spectrum for $T_{\rm eff}$ = 3900 K, log (g[cm/s^2]) = 1.0, solar mass and chemical abundances (dashed line). A wavelength range including the V = 4 $\rightarrow$ 2 bandhead of ^{28}SiO and another one, which is situated in a region between two bandheads, are shown.

If one wants to study the fundamental transition bands of SiO, the existing observational data are only poor. This is caused by the fact that up to now it was very difficult to obtain spectra of the wavelength range around 8 μm with ground based telescopes. As a consequence many of the measurements come from space- or airborne instruments. Cohen et al. (1992) have published mid infrared spectra for K and early M giants obtained with the Kuiper Airborne Observatory. They found that all objects including even the hottest ones with a spectral type of K1 III (α Boo) show a considerable SiO absorption at 8 μm. The features become stronger, if one goes from K to M stars. These results and a rough estimation of the observed band intensities agree with our models. On the other hand Vardya et al. (1986) report the detection of SiO emission in the IRAS LRS spectra of several Mira variables. Of course, such a behavior can not be explained by our classical model atmospheres, which produce strong fundamental absorption bands for very cool and extended stars. Thus, we might face a similar situation as for the first overtone transitions in AGB objects, where the observed absorption features are much weaker than the predicted ones. This could also be caused by some additional emission, as it was proposed by Tsuji et al. (1994). However, any identification of the fundamental bands based only on IRAS LRS spectra should be regarded as uncertain. First they are situated close to the blue edge of the reliable part of the LRS spectra (Joint IRAS Science Working Group 1988) and second the 9.7 μm silicate dust feature extends into the corresponding wavelength range (Simpson 1991), both making a definition of the continuum very difficult.

5. Conclusions

We have computed a grid of model atmospheres and spectra focusing on the effects and appearance of the SiO bands. It was shown that the latter never have a large influence on the atmospheric structure, at least as long as one stays within the framework of classical hydrostatic calculations using equilibrium chemistry. In addition we have demonstrated that the intensity of the absorption features monotonously increases with lower temperature and gravitational acceleration as well as with higher metallicity. Thus, from the models we expect the strongest bands in the coolest and most extended objects, whereas they will almost disappear in dwarfs with $T_{\rm eff} > 4000$ K and in giants with $T_{\rm eff} > 4800$ K, if solar chemical abundances are assumed.

When we compared our results to existing observations of K and early M giants, we found that there is a good agreement indicating the correctness of the adopted line data and atmospheres. Nevertheless, the calculations fail completely in predicting the band intensities of AGB objects. We think that this is caused by the fact that our classical model atmospheres can not always be applied to this kind of stars and some basic assumptions like hydrostatic and chemical equilibrium may not work anymore as it is indicated by the observed strong variability of the SiO absorption. In addition atmospheric inhomogenities (e.g. Olofsson et al. 1996) and SiO emission might become important. Some of the aspects will be discussed in the second paper of this series, where we will focus on our observations of AGB stars and the impact of dynamical phenomena like stellar pulsation, shock waves, mass loss and dust formation based on existing models (e.g. Höfner & Dorfi 1997) and our synthetic spectra.

Acknowledgements. We thank K. Hinkle and T. Lebzelter for helping us to access the FTS data of several red giants and J. Hron for valuable suggestions. Part of this work was supported by the Austrian Science Fund Project S7308–AST. The necessary computing facilities were made available through support from the Carlsberg Foundation. We acknowledge travel support from the Danish Natural Science Research Council.

References

Anders E., Grevesse N., 1989, Geochimica et Cosmochimica Acta 53, 197
Aringer B., Wiedemann G., Käufl H.U., Hron J., 1995, Ap&SS 224, 419
Blackwell D.E., Petford A.D., Arribas S., Haddock D.J., Selby M.J., 1990, A&A 232, 396
Bonnell J.T., Bell R.A., 1993, MNRAS 264, 319
Cohen M., Witteborn F.C., Carbon D.F., et al., 1992, AJ 104, 2045
Cuntz M., Muchmore D.O., 1994, ApJ 433, 303
Di Benedetto G.P., Rabbia Y., 1987, A&A 188, 114
Drake J.J., Smith G., 1991, MNRAS 250, 89
Elitzur M., 1992, Astronomical Masers, Kluwer Academ. Publishers
Gail H.P., Sedlmayr E., 1986, A&A 166, 225
Grevesse N., Sauval A.J., 1994, Proc.: Molecules in the Stellar Environment, IAU Colloquium 146, ed. U.G. Jørgensen, Springer-Verlag (Lecture Notes in Physics 428), p. 196
Gustafsson B., Bell R.A., Eriksson K., Nordlund Å., 1975, A&A 42, 407
Gustafsson B., Jørgensen U.G., 1994, A&AR 6, 19
Hinkle K.H., Barnes T.G., Lambert D.L., Beer R., 1976, ApJ 210, L141
Höfner S., Dorfi E.A., 1997, A&A 319, 648
Joint IRAS Science Working Group, 1986, IRAS Catalogs and Atlases, IRAS Atlas of low-resolution Spectra, A&AS 65, 607
Joint IRAS Science Working Group, 1988, IRAS Catalogs and Atlases, Vol. 1, Explanatory Supplement, eds. C.A. Beichman, G. Neugebauer, H.J. Habing, P.E. Clegg, T.J. Chester, NASA RP–1190
Jørgensen U.G., 1992, Rev. Mexicana Astron. Astrof. 23, 195
Jørgensen U.G., 1994a, A&A 284, 179
Jørgensen U.G., 1994b, Proc.: Molecules in the Stellar Environment, IAU Colloquium 146, ed. U.G. Jørgensen, Springer-Verlag (Lecture Notes in Physics 428), p. 29
Jørgensen U.G., Johnson H.R., Nordlund Å., 1992, A&A 261, 263
Lambert D.L., 1994, Proc.: Molecules in the Stellar Environment, IAU Colloquium 146, ed. U.G. Jørgensen, Springer-Verlag (Lecture Notes in Physics 428), p. 1
Langhoff S.R., Bauschlicher C.W., 1993, Chem. Phys. Lett. 211, 305
Muchmore D.O., Nuth J.A., Stencel R.E., 1987, ApJ 315, L141
Nordlund Å, 1984, In: Methods in Radiative Transfer, ed.: W. Kalkofen, Cambridge University Press, Cambridge, p. 211
Olofsson H., 1988, Space Science Reviews 47, 145
Olofsson H., Bergman P., Eriksson K., Gustafsson B., 1996, A&A 311, 587
Ridgway S.T., Jacoby G.H., Joyce R.R., Siegel M.J., Wells D.C., 1982, AJ 87, 1044
Ridgway S.T., Carbon D.F., Hall D.N.B., Jewell J., 1984, ApJS 54, 177
Rinsland C.P., Wing R.F., 1982, ApJ 262, 201
Rossi S.C.F., Maciel W.J., Benevides-Soares P., 1985, A&A 148, 93
Sahai R., Bieging J.H., 1993, AJ 105, 595
Sauval A.J., Tatum J.B., 1984, ApJS 56, 193
Simpson J.P., 1991, ApJ 368, 570
Tsuji T., Ohnaka K., Hinkle K.H., Ridgway S.T., 1994, A&A 289, 469
Vardya M.S., De Jong T., Willems F.J., 1986, ApJ 304, L29

This article was processed by the author using Springer-Verlag LaTeX A&A style file *L-AA* version 3.